



## Original article

## Molecular design and synthesis of HCV inhibitors based on thiazolone scaffold



Ghada H. Al-Ansary<sup>a</sup>, Mohamed A.H. Ismail<sup>a,\*\*</sup>, Dalal A. Abou El Ella<sup>a</sup>, Sameh Eid<sup>b</sup>,  
Khaled A.M. Abouzid<sup>a,\*</sup>

<sup>a</sup> Pharmaceutical Chemistry Department, Faculty of Pharmacy, Ain Shams University, Cairo 11566, Egypt

<sup>b</sup> Institute of Molecular Pharmacy, Pharmazentrum, University of Basel, Switzerland

## ARTICLE INFO

## Article history:

Received 2 March 2013

Received in revised form

8 July 2013

Accepted 15 July 2013

Available online 24 July 2013

## Keywords:

HCV

Thiazole

Glide docking

HCV NS5B inhibitor

Sulfonamide derivatives

## ABSTRACT

A series of thiazolone derivatives was designed and synthesized as potential HCV NS5B allosteric polymerase inhibitors at the allosteric site thumb II. Their antiviral activity was evaluated and molecular modeling was utilized to give further envision on their probable binding modes in the allosteric binding site. Among the tested molecules, compound **9b** displayed sub-micromolar inhibitory activity with an  $EC_{50}$  of 0.79  $\mu$ M indicating excellent potency profile. It also showed good safety profile ( $CC_{50} \geq 75 \mu$ M and  $SI \geq 94.3$ ).

© 2013 Elsevier Masson SAS. All rights reserved.

## 1. Introduction

Hepatitis C virus is a meticulous factor of liver disease and one of the most important health issues worldwide [1]. HCV has approximately 175 million Global Disease Burden which represents almost 3% of the whole population in the world. Each year 3–4 million new patients with HCV are diagnosed [2,3]. This disease will continue to be a serious global health threat for many years to come because of the chronic nature of the infection, its high prevalence, and the significant morbidity of the resulting disease [4].

Among all HCV infected individuals, 85% of them remain chronically infected, thus, 15% will undergo spontaneous clearance. 10%–20% of those chronically infected develop cirrhosis (a scarring of the liver), and 1%–5% of them acquire liver cancer over years [5,6]. The risk for developing cirrhosis 20 years after initial HCV infection is estimated at around 10%–15% for men and 1%–5% for women. Once cirrhosis is established, the rate of developing hepatocellular carcinoma (HCC) is at 1%–4% per year. Approximately 280,000 deaths worldwide per year are related to HCV infection

[7–9]. HCV related end-stage liver disease and HCC have become the leading cause for liver transplantation worldwide [10–12].

The current standard of care (SoC) for HCV infection consists of a combined therapy of injectable pegylated interferon alfa (pegIFN- $\alpha$ ) and ribavirin administered for 24–48 weeks depending on the HCV genotype [13,14]. However, this therapy has many limitations, being long, expensive, toxic, and only effective in around 50% of the patients for the most common genotype [15,16]. Moreover, SoC therapy is not suitable for people suffering from severe HCV related cirrhosis, undergone organ transplant, children of <3 years and specific contraindication to the medication [17]. For such a therapy, patient compliance is quite questionable. With an escalating number of patients who are infected with HCV for more than 15 years, many of whom are likely to develop advanced liver diseases by 2012, there remains an urgent unmet need for more-effective, less-toxic, and less-complex treatment regimens with shorter durations.

The NS5B RNA-dependent RNA polymerase (RdRp) is the central enzyme that is responsible for replication of the viral genome, and has since become a target of choice for the screening and design of small molecular inhibitors, which in principle, should interfere with viral replication [18]. This biochemical activity has no known mammalian equivalent, offering the opportunity to identify very selective inhibitors of viral enzyme. Different allosteric sites on HCV

\* Corresponding author. Tel.: +20 1222165624; fax: +20 25080728.

\*\* Corresponding author. Tel.: +20 1223269674.

E-mail addresses: [mhismaeel@yahoo.com](mailto:mhismaeel@yahoo.com) (M.A.H. Ismail), [Khaled.abouzid@pharm.asu.edu.eg](mailto:Khaled.abouzid@pharm.asu.edu.eg), [abouzid@yahoo.com](mailto:abouzid@yahoo.com) (K.A.M. Abouzid).

NS5B have been identified, both at the palm and thumb domains. Various institutions and pharmaceutical companies have reported structurally diverse molecular inhibitors of NS5B, some of them have successfully entered phase II clinical trials [19–22]. Thus NS5B RdRp is a very tractable drug discovery target.

Recently, several non-nucleoside inhibitors (NNIs) bearing a thiazole ring have been identified, optimized and biologically evaluated for their anti-HCV activity. As many of them showed subnanomolar activity, this tempted us to find other mechanistically unique scaffolds [19,21,22].

Several scaffolds have been reported to bind several of the allosteric binding sites of NS5B, which are located on the thumb sub-domains distant from the polymerase active site. Inhibitors bound to such allosteric sites of enzymes are generally considered to have fewer off-target side effects than nucleoside analogs due to absence of binding to homologous cellular enzymes [23].

One of our endeavors in HCV programs was aimed to discover novel thiazole derivatives as candidate molecules that can bind to the allosteric site of HCV NS5B designated as “Thumb pocket II”.

Based on the previous SAR and molecular modeling studies, we were endeavored to design, synthesize and biologically evaluate a novel series of thiazole derivatives aiming to reach successful candidates as HCV polymerase inhibitors.

Our structure-based design strategies for new scaffolds were based on the diversification of initial hit **1** revealed by Valeant Pharmaceuticals in 2006 with an  $IC_{50}$  value of 2.0 against HCV NS5B. X-ray soaking experiments which revealed that it was bound in a binding pocket which is on the protein's surface 30 Å away from the enzyme's catalytic center, designated as “Thumb pocket II” [24]. Our design strategy for new scaffolds is three folds: i. identification of the key interactions with the binding site, ii. exploration of previous revealed SAR studies, and iii. diversification of the structure with retention of the essential pharmacophoric groups in order to identify further new scaffolds favoring the selectivity.

X-ray complex structure from soaking experiments of the reported thiazolone hit compound ( $IC_{50} = 2.0 \mu M$ ), established its binding mode in the allosteric site (PDB code 2HWH). Key interactions include [24]: C=O, N of the thiazole ring and sulfonamide moiety form H-bonds with backbone –NHs of Tyr477, Ser476 and the basic side chain –NH<sub>3</sub><sup>+</sup> of Arg501, respectively, while, the furan and the phenyl rings make hydrophobic contacts with the side chains of Leu 419, Met423, Ile 482, Val485, Leu489, Leu497, and Trp528 of the protein.

Additionally, as previously reported [25], close examination of the inhibitor–protein interactions revealed that in the vicinity of these inhibitor-binding interactions there seems to be an additional pocket that still needs further exploration. For our information, the entrance of this pocket is flanked by two basic amino acid residues, His475 and Lys533 [25]. Accordingly, Yan et al. concluded that an inhibitor properly designed to interact with these two amino acid residues could represent a new molecular platform for probing this extra pocket.

SAR studies conducted on a large number of thiazolone derivatives of hit **1**, revealed the following [26,27]: i. A furan moiety coupled to a thiazolone core by  $sp^2$ -hybridized carbon linker is essential for activity. ii. Replacement of the furan moiety with phenyl groups extended with both aromatic and non-aromatic heterocycle at the para position resulted in potency improvement. iii. Replacement of the furan moiety with a pyridyl group linked to the thiazolinone ring resulted in marked increase in potency. iv. N-alkylation of the sulfonamide afforded compounds which do not have interesting activities. v. The acidic moiety is critical for activity as the replacement of the sulfonamide with an amide afforded compounds with lower activities. vi. Substitution of the phenyl ring with halogens or other hydrophobic groups increased the potency.

### 1.1. Bioisosteric modifications

Thus, our structure-based design strategies aimed at identifying the possible opportunities of diversification and optimization with retention of the pharmacophoric groups of the lead compound revealed by SAR study and X-ray soaking experiments. Accordingly, a new series of molecules was designed based on modification of the left part of the molecule by introducing different arylidene moieties in place of the furyl ring, whereas, concomitant introduction of different substituents on the phenyl ring brought modification of the right portion of the molecule (Fig. 1).

Moreover, as a continuum of our design strategy, we were motivated to design a molecule that can interact specifically with the two basic amino acid residues His475 and Lys533 near the entrance of the hydrophobic pocket to probe for extra binding with the enzyme. We envisioned that a design of such a new scaffold would constitute three iterative steps (Fig. 1). First, a fragment template (part I) was selected as an anchor to the binding site for the purpose of establishing the same interactions with the protein as that of hit **1**, obviously it bears its same pharmacophoric groups. Second, an acetylpiperazinyl spacer (part II) was introduced so that the molecule elongates to reach the entrance of the hydrophobic pocket. The design was completed by connecting an aromatic methoxyphenyl moiety (part III) to the other side of the linker in order to pick up a seemingly aromatic  $\pi$ – $\pi$  stacking with the hydrophobic pocket.

## 2. Results and discussion

### 2.1. Chemistry

Sulfonamides **6a–i** and **7a, b** were prepared by the condensation of the key intermediates **4a–c** with different aldehydes in a refluxing mixture of glacial acetic acid and anhydrous sodium acetate. An alternative procedure was applied for the synthesis of the titled molecules **6a–i**, where the intermediates **5a–d** were reacted with 4-substituted-benzenesulfonyl chloride derivatives in refluxing THF using TEA as a base (Schemes 1 and 2). The former procedure afforded the titled compounds **6a–i** in a better yield (64–81% vs. 45–60%).

The structures of the titled compounds were confirmed by spectral and analytical data. The FT-IR spectra revealed a broad peak for the NH of the sulfonamide group ranging from  $3450 \text{ cm}^{-1}$  to  $3080 \text{ cm}^{-1}$ . Their <sup>1</sup>H-NMR spectra showed a singlet corresponding to the olefinic proton ranging from  $\delta$  7.58 ppm to  $\delta$  7.89 ppm. Moreover, their EIMS spectra showed molecular ion peaks corresponding to the molecular weight of each compound, further confirming their structures.

The titled compounds **8a, b** were synthesized by acid hydrolysis of the intermediates **7a, b**. This was done by refluxing **7a, b** in 2 N HCl for 2 h in order to avoid the hydrolysis of the less active sulfonamide group.

The structures of the titled compounds were proved by analytical and spectral data. The FT-IR spectra revealed a forked peak at  $3280 \text{ cm}^{-1}$  and  $3120 \text{ cm}^{-1}$  for compounds **8a** and **8b**, respectively, corresponding to the primary amino group. Their <sup>1</sup>H-NMR showed the appearance of a broad singlet integrated to two protons (–NH<sub>2</sub>) at  $\delta$  12.73 ppm and  $\delta$  9.42 ppm for **8a** and **8b**, respectively. Their EIMS spectra showed molecular ion peaks at  $m/z$  394 and 435, respectively, corresponding to their molecular weights, which further confirmed their structures.

In the current study, the titled compounds **9a, b** were prepared by N-alkylation of the key intermediates **8a, b** with 1-(2-chloroacetyl)-4-(2-methoxyphenyl)piperazine in K<sub>2</sub>CO<sub>3</sub> and acetone (Scheme 2). The <sup>1</sup>H-NMR of these final products **9a, b**, revealed the existence of the additional characteristic singlets for

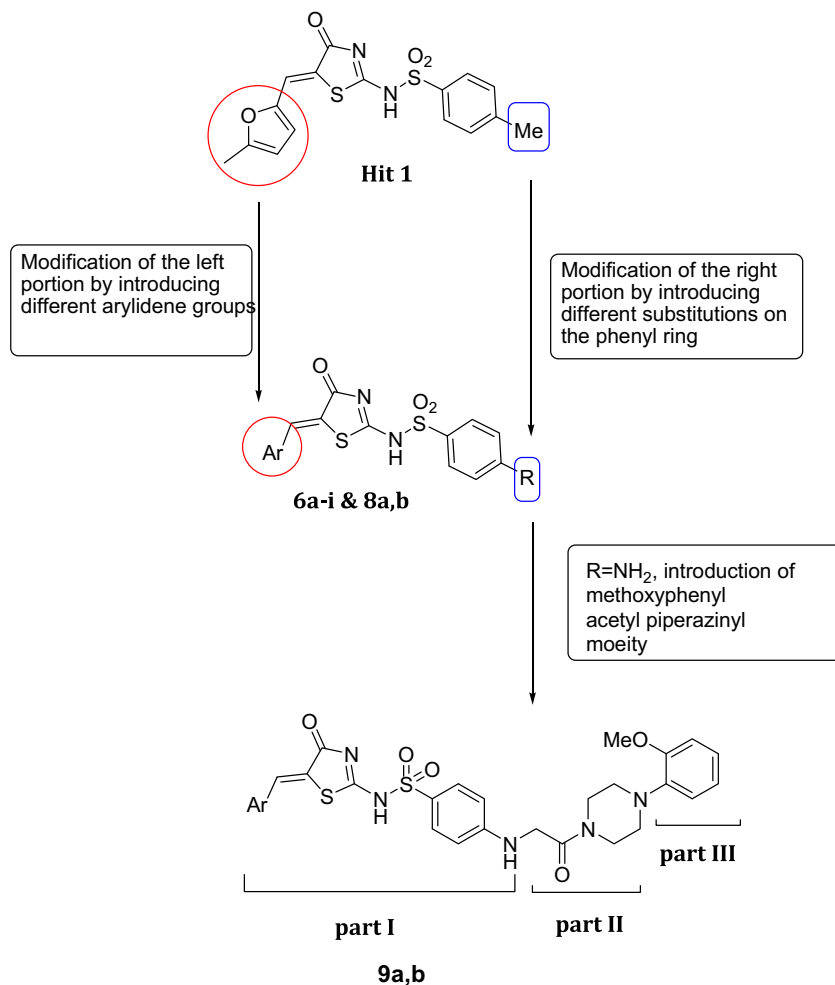


Fig. 1. Structure-based design of HCV NS5B allosteric-site inhibitors **6a–i** & **8a, b**.

(–CH<sub>2</sub>–CO–) at  $\delta$  4.66 ppm and  $\delta$  4.69 ppm, respectively, as well as the two multiplet signals of the piperazine protons (–N–CH<sub>2</sub>–CH<sub>2</sub>–N–) at  $\delta$  3.61–3.55 ppm and  $\delta$  3.05–2.91 ppm for **9a** and at  $\delta$  3.68–3.50 ppm and  $\delta$  3.02–2.93 ppm for **9b**. The EIMS of the obtained products **9a, b** showed molecular ion peaks at  $m/z$  626 and 667 which is consistent with their molecular weights.

## 2.2. Biological evaluation

Through analysis of the biological activities of the test compounds shown in (Table 1), we can deduce the following by scrutinizing their EC<sub>50</sub>, CC<sub>50</sub>, SI and %Max values.

### 2.2.1. In the sulfonamide series (**6a–i**)

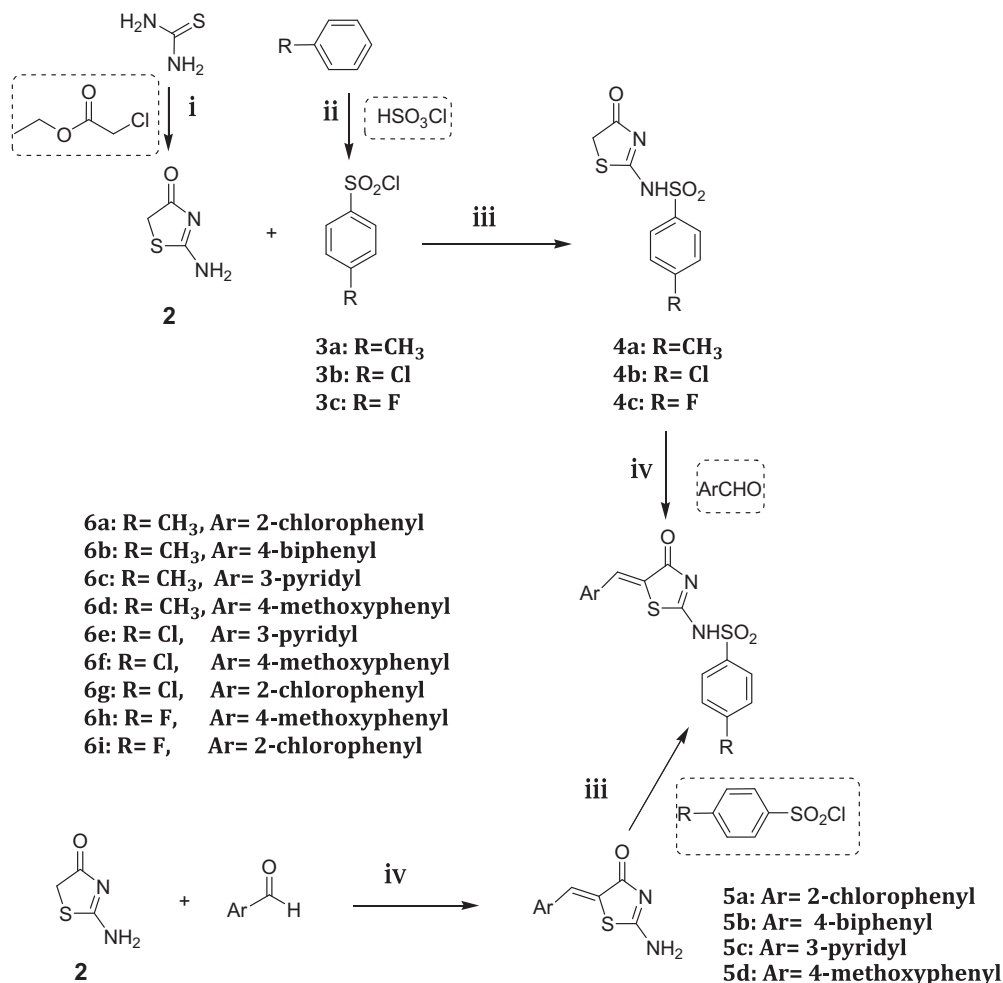
Among the 9 new test compounds, 3 of them (compounds **6d**, **6f**, and **6i**) demonstrated moderate inhibitory activity (50%) of the HCV subgenomic replication in the Huh 5-2 cell line. But, unfortunately, this was associated with marked cellular toxicity which hampered the determination of any EC<sub>50</sub> values for them.

The sulfonamides (**6a–c**, **6e**, **6g**, and **6h**) were found to inhibit HCV sub-genomic replicon replication with potency (EC<sub>50</sub> = 16.63  $\mu$ M–74.74  $\mu$ M) and exhibited low toxicity (CC<sub>50</sub> = 68.04  $\mu$ M–>140  $\mu$ M), in addition to their SI values (1.19–>8.37) which further confirmed their tolerable cytotoxicity profile. Unfortunately, for compounds **6a** and **6h**, the SS values of these compounds revealed a detrimental “overall antiviral activity”.

Although compound **6b** showed good cellular activity (EC<sub>50</sub> = 58.75) and toxicity profile (CC<sub>50</sub>  $\geq$  115 and SI  $\geq$  1.96), along with a maximum percentage inhibition of 69.3%, yet, the most appealing results were associated with sulfonamides (**6c**, **6e** and **6g**). These demonstrated potent anti-HCV activities of EC<sub>50</sub> values of 16.63  $\mu$ M, 64.11  $\mu$ M and 48.90  $\mu$ M, individually, which was further confirmed by the percentage of the maximum inhibitory effect they produced (87.5%, 74.6%, and 69.9%). Furthermore, although no EC<sub>90</sub> values were obtained for any of them, yet, an EC<sub>70</sub> of 55.71  $\mu$ M was obtained for compound **6c**. The cytotoxicity profile of the three compounds, designated by CC<sub>50</sub> values of >140  $\mu$ M, >132  $\mu$ M, and >121  $\mu$ M showed low or no detected toxicity within the experimental range. This was further confirmed by the SI values of >8.37, >2.06, and >2.48. Furthermore, the SS values of >15.9, >8.86, and >3.02, indicated an excellent “overall antiviral potency”. The interpretation of their dose–response curves revealed that they have selective (genuine) antiviral activity.

### 2.2.2. In the sulfanilamide series (**8a, b** and **9a, b**)

Luciferase assay performed on compounds (**8a, b** and **9a, b**) revealed that all test compounds except for **8b** demonstrated inhibitory activity on HCV RNA replication (EC<sub>50</sub> values of 95.67  $\mu$ M, 22.68  $\mu$ M, and 0.79  $\mu$ M, respectively), whereas the MTS-based assay proved that they lack cytotoxicity within the experimental range. Comparing the cellular potencies of compounds **8a, b** which bear the polar para-amino group with those of compounds **9a, b** whose



**Reagents and conditions:** i. 95% Ethanol, reflux, 3h. ii. 0°C, 4h. iii. THF, TEA, reflux, 48h. iv. Anhydrous sodium acetate, glacial acetic acid, reflux, 16h.

**Scheme 1.** Synthesis of (Z)-2-arylsulfonamido-5-(arylmethylene) thiazol-4-(5H)-ones (**6a–i**).

amino group is substituted with a basic piperazinyl moiety which bears a large hydrophobic *o*-methoxyphenyl group at its end, provides guidelines for useful structure–activity relationship information.

Compounds **9a, b** (EC<sub>50</sub> = 22.68 μM, and 0.79 μM) are much more potent than their corresponding unsubstituted amines **8a, b** (EC<sub>50</sub> = 95.67 μM and >115 μM) along with a marked increase in the maximum percentage inhibition of **9a, b** (76.5% and 88.5%) over those of **8a, b** (58% and 13.1%).

This result indicates that the polar para-amino group in compounds **8a, b** may be problematic for cellular permeability. However, replacing it with a basic piperazine moiety which bears a large hydrophobic *o*-methoxyphenyl group resulted in **9a, b**, that are molecules combining good replicon potency and good pharmacokinetics. This may be due to an extra interaction of the hydrophobic substituted aromatic ring with the amino acid residues of the binding site.

Compound **9b** was the best compound identified, with an EC<sub>50</sub> of 0.79 μM indicating excellent potency profile. It also showed good safety profile (CC<sub>50</sub> ≥ 75 μM and SI ≥ 94.3). The value of the SS was calculated to be >52.5 which further confirms that it has a good “overall antiviral potency”. The interpretation of its dose–response curve revealed that it has selective (genuine) antiviral activity.

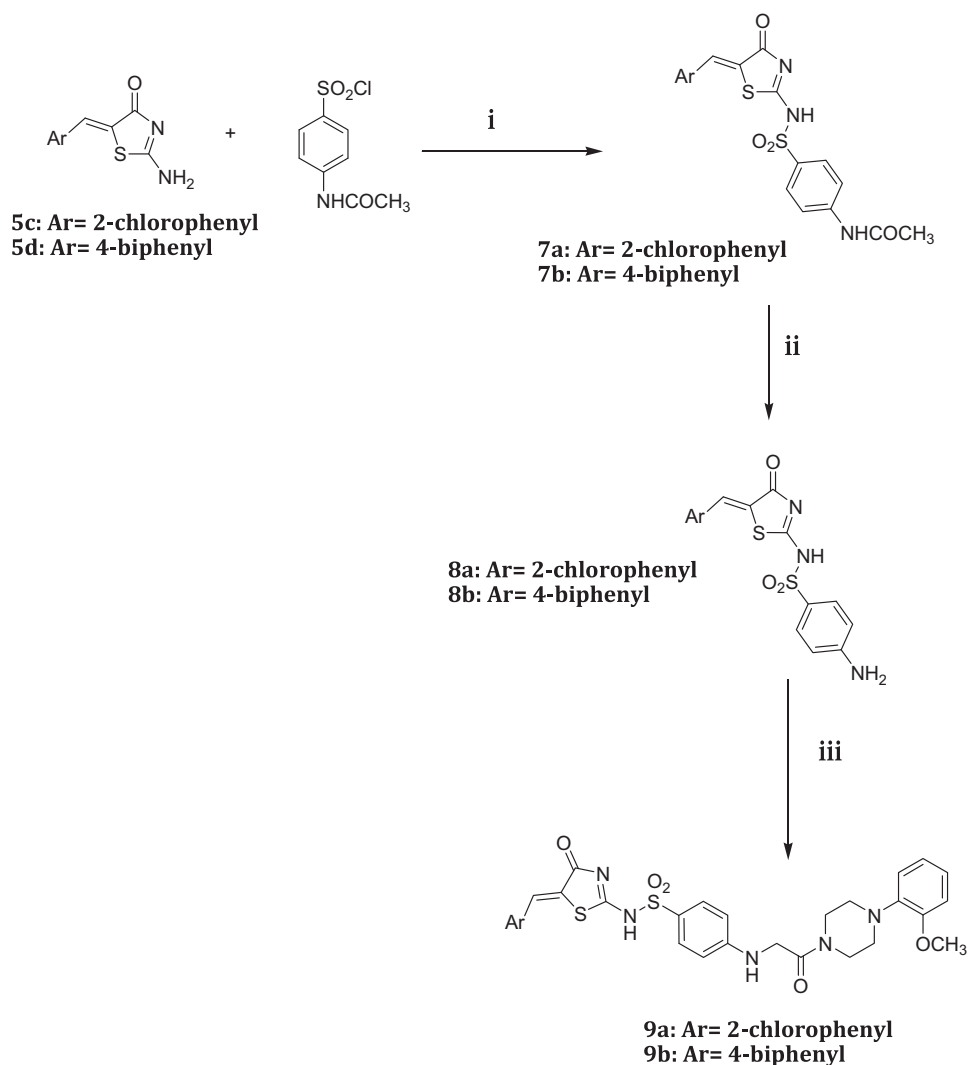
### 3. Molecular modeling

#### 3.1. Validation of Glide docking on HCV NS5B

Several crystal structures of HCV NS5B bound to thumb site II allosteric inhibitors were solved. For instance, Yan and co-workers reported crystal structures for HCV NS5B polymerase in complex with four different thiazolone derivatives (**1–4**) [24,25,27] (Table 2).

Each of these complexes was subjected to a *self*-docking run to validate the proposed docking methodology. In such runs the co-crystallized ligand is removed from the complex, docked back into the binding site and then heavy-atom RMSD to reference pose are calculated. A docking simulation is described as *successful* if one (or more) of the top-ranked output poses exhibits RMSD lower than 2.0 Å to the experimentally solved pose.

In all cases, heavy-atom RMSD values between top-ranked pose(s) and experimental crystal structure were lower than 1.7 Å (Table 2). Moreover, in most cases the first-ranked pose or one of the three top-ranked poses exhibited RMSD values lower than 0.7 Å (Fig. S1, Supporting Information). Glide, thus, seems to be appropriate for reliable prediction of docking poses for our compounds. All docking scores and interaction fingerprints for modeled compounds are shown in (Table 3).



**Reagents and conditions:** i. THF, TEA, reflux, 24h. ii. 2 N HCl, reflux, 2h. iii. 1-(2-Chloroacetyl)-4-(2-methoxyphenyl)piperazine, acetone, anhydrous  $K_2CO_3$ , reflux, 24h.

**Scheme 2.** Synthesis of (Z)-4-aminophenylsulfonamido-5-(arylmethylene)thiazol-4(5H)-one (**8a**, **b**) & (Z)-N-(5-Arylmethylene-4-oxo-4,5-dihydrothiazol-2-yl)-4-(2-(4-(2-methoxyphenyl)piperazin-1-yl)-2-oxoethylamino)benzenesulfonamide (**9a**, **b**).

### 3.2. Sulfonamide series (compounds **6a–i**)

All sulfonamides series (**6a–i**) demonstrated very similar binding poses, where backbone NH's of Ser476 and Tyr477 were involved in H-bonds with thiazoline ring nitrogen and carbonyl group, respectively. Sulfonamide oxygens impart favorable electrostatic interactions with side chains of Arg501 and Lys533 as seen in reported sulfonamide inhibitors (Fig. 2). Finally, the aromatic moiety linked to sulfonamide group pointed towards hydrophobic sub-pocket A (Leu419, Met423 and Trp528), while the second aromatic moiety *partially filled* hydrophobic sub-pocket B (Ile482, Val485, Leu489, Pro496 and Leu497).

Hydrophobic sub-pocket B seems to be large enough to accommodate even bigger substituents (e.g. biphenyl in compound **6b**) without compromising the crucial hydrogen-bonding between thiazoline ring and backbone NH's of Ser476 and Tyr477 (Fig. 5) (Fig. S2, Supporting Information). Keeping in mind the versatility of the hydrophobic sub-pockets, it's not surprising to find out that the nature of aromatic moieties and their substituents in the studied

**Table 1**

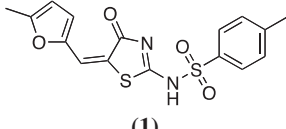
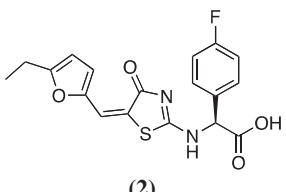
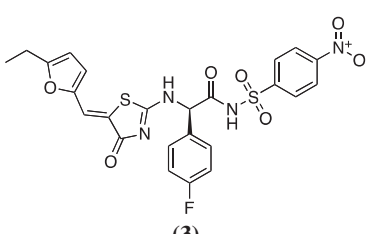
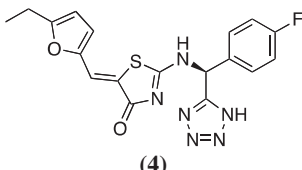
EC<sub>50</sub>, CC<sub>50</sub>, SI, SS, Max% and [ ] Max for the test compounds assayed for their anti-HCV activity (genotype 1b) and cell viability.

Cpd. no	EC <sub>50</sub> (μM)	CC <sub>50</sub> (μM)	SI	SS	Max%	[ ] Max (μM)
6a	44.02	76.10	1.73	0.0329	61.8	77.09
6b	58.75	>115	>1.96	>3.03	69.3	91.70
6c	16.63	>140	>8.37	>15.9	87.5	140
6d	ND	68.04	ND	0	50	68.04
6e	64.11	>132	>2.06	>8.86	74.6	132
6f	ND	71.07	ND	0	50	71.07
6g	48.90	>121	>2.48	>3.02	69.9	121
6h	74.74	88.77	1.19	0.0986	54.5	98.21
6i	ND	115	ND	ND	49.8	126
8a	95.67	>127	>1.33	>0.55	58	120
8b	>115	>115	ND	ND	13.1	22.98
9a	22.68	>80	>3.52	>7.98	76.5	62.93
9b	0.79	>75	>94.3	>52.5	88.5	15.73



**Table 2**

Self-docking results for HCV NS5B complexes with selected thumb site II inhibitors. Root-mean-squared-distance between top-ranked poses from automated docking and experimental geometry confirms the reliability of the employed docking procedure.

PDB code	Ligand structure	Resolution	RMSD of top-ranked pose(s)
2HWH	 (1)	2.3 Å	0.97–1.11 Å
2HWI	 (2)	2.0 Å	0.67–1.64 Å
205D	 (3)	2.2 Å	1.20–1.26 Å
211R	 (4)	2.2 Å	0.66–1.26 Å

compounds had little or no influence on their orientations in the binding site, nor their docking scores (Fig. 6) (Fig. S3, Supporting Information).

In addition to the expected docking pose (Fig. 3, left), compound **6g** exhibited a different binding mode where the thiazoline ring is inverted, thus losing an H-bond with Tyr477 NH. This loss is – at least in part – compensated by a strong H-bond to Lys533 side chain NH<sub>3</sub><sup>+</sup> and a face–face stacking of one aromatic moiety with His475 side chain (Fig. 3, right). However, this re-orientation also leads to loss of hydrophobic interactions with hydrophobic sub-pocket B.

On the other hand, compounds **6h** and **6i**, as expected, exhibit the same orientation seen in the co-crystallized ligands (Fig. S4, Supporting Information).

### 3.3. Sulfanilamide series (compounds **8a**, **b** and **9a**, **b**)

All docking poses retrieved from Glide docking of compounds **9a** and **9b** to the rigid receptor (Fig. 5) showed that neither of them could bind in a manner similar to their un-substituted amino analogs **8a** and **8b**, respectively (Fig. 4). In both compounds the thiazoline ring is far from its typical binding site near backbones of Ser476 and Tyr477. In **9a** the thiazoline substituent is pointed towards hydrophobic sub-site A, while the long amino substituent

**Table 3**

Docking scores and interaction fingerprints for the docking poses of modeled compounds; residues defining interaction sub-sites are given below the table.

Cpd no.	EC <sub>50</sub> (μM)	G_Score (kcal/mol)	Polar sub-site	Hyd.A	Hyd.B
<b>6a</b>	44.02	−6.07	−19.04	−10.43	−8.03
<b>6b</b>	58.75	−6.13	−18.36	−11.66	−12.14
<b>6c</b>	16.63	−6.26	−19.04	−10.43	−8.03
<b>6d</b>	ND	−5.97	−17.56	−14.31	−9.97
<b>6e</b>	64.11	−5.70	−13.64	−11.14	−3.54
<b>6f</b>	ND	−6.19	−15.35	−10.92	−6.99
<b>6g</b>	48.90	−5.29	−15.67	−11.12	−7.13
<b>6h</b>	74.74	−6.57	−16.41	−10.51	−9.86
<b>6i</b>	ND	−6.19	−16.27	−11.39	−8.26
<b>8a</b>	95.67	−5.77	−19.37	−11.30	−7.87
<b>8b</b>	>115	−5.94	−18.17	−11.48	−12.49
<b>9a</b>	22.68	−6.19	−24.78	−10.60	−7.76
		−4.50 <sup>a</sup>	−21.13 <sup>a</sup>	−4.90 <sup>a</sup>	−8.82 <sup>a</sup>
		−8.75 <sup>b</sup>	−42.99 <sup>b</sup>	−9.13 <sup>b</sup>	−9.30 <sup>b</sup>
<b>9b</b>	0.79	−5.14	−16.16	−10.82	−2.24
		−4.70 <sup>a</sup>	−17.88 <sup>a</sup>	−7.75 <sup>a</sup>	−9.21 <sup>a</sup>
		−8.47 <sup>b</sup>	−26.47 <sup>b</sup>	−12.58 <sup>b</sup>	−10.14 <sup>b</sup>
		−6.89 <sup>b</sup>	−27.6 <sup>b</sup>	−10.19 <sup>b</sup>	−8.80 <sup>b</sup>

Polar sub-site:  $\Sigma$ (Ser476, Tyr477, Arg501, Lys533).

Hyd.A (hydrophobic sub-site A):  $\Sigma$ (Leu419, Met423 and Trp528).

Hyd.B (hydrophobic sub-site B):  $\Sigma$ (Ile482, Val485, Leu489, Pro496 and Leu497).

<sup>a</sup> Semi-automated constrained docking.

<sup>b</sup> Induced-fit docking.

fills sub-site B; the opposite was observed in compound **9b**. In both cases, however, hydrophobic substituents are accommodated less optimally in the binding site than the respective un-substituted amines.

In order to explain the inability of compounds **9a** and **9b** to maintain the reported binding mode of NS5B polymerase inhibitors, another semi-automated docking run was setup. In that special docking run, a soft constraint was added so as to force Glide to place the thiazoline ring close to its position in typical inhibitors. In effect, Glide was allowed only to vary and optimize the positioning of the two hydrophobic tails. As demonstrated in (Fig. 6), the p-methoxyphenyl-piperazinyl side chain is too big to fit in the relatively tight hydrophobic sub-pocket A. Alternatively; significant twisting at the sulfonamide group was necessary to avoid placing the piperazinyl tail where it clashes with the receptor. This leads to a strained conformation that almost totally lost all interaction with sub-pocket A, only slightly compensating this by weaker interactions with e.g. Pro479. Straining, loss of hydrophobic interactions coupled with non-optimal H-bonding with Ser476/Tyr477 pair leads to a substantially lower score being assigned to these poses, which in turn explains why automated docking discarded them previously. An extensive induced-fit docking would, thus, seem to be necessary for both compounds to give a better picture of their possible binding modes taking into account re-adjustment of binding site residues side chains as explained in methodology. In the top-ranked pose of **9a** hydrogen bonding to Ser476/Tyr477 pair was taken over by NH and carbonyl groups of the linker (Fig. 7, left). Compound **9b** exhibited a similar pose to that of **9a** (Fig. 7, right), in addition to another lower score pose which looks like the typical binding mode with a slightly shifted thiazoline ring engaging only one hydrogen bond to backbone NH of Ser476 (Fig. 8). Additionally, significant conformational change took place in the side chain of Arg501 to allow for H-bond to carbonyl group of the linker and avoid clashes with piperazinyl tail. The lower score of this mode could be attributed to the factors discussed above; namely, higher internal strain, weaker H-bond to key residues and weak or no interaction with sub-pocket A.

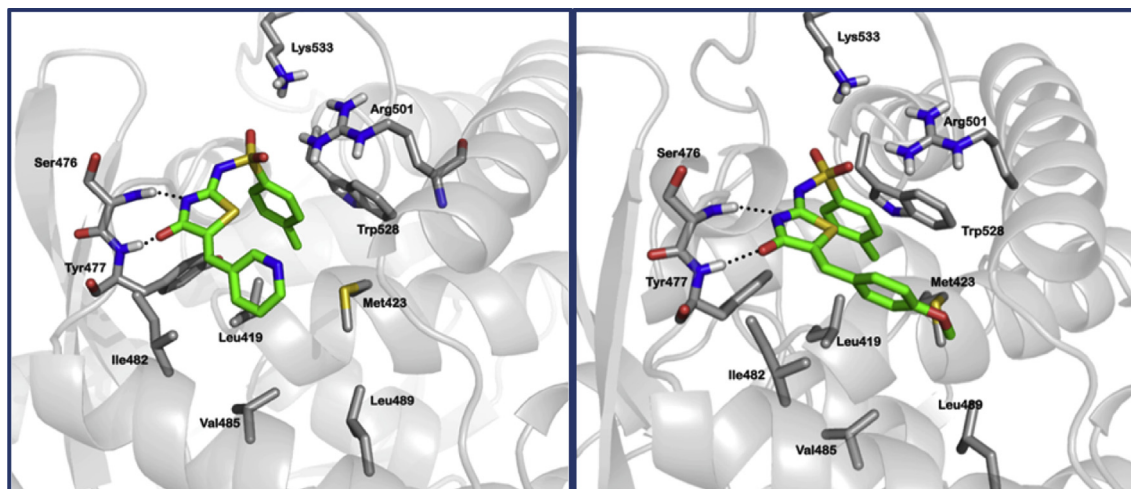


Fig. 2. Top-ranked docking poses for sulfonamides **6a** (left) and **6b** (right).

#### 4. Conclusion

The antiviral activity of the target compounds was evaluated and molecular modeling was used to give further envision about their probable binding modes in the allosteric binding site.

Analyzing the  $EC_{50}$  values for the tested compounds and exploring their different binding modes in the binding pocket, taking into consideration their docking scores, we can come to the following SAR conclusion:

- i. Modification of the left part of the thiazolone scaffold (series **6**) did not result in significant variation of the biological activity. The nature of the aromatic moieties and their substituents (**6a** vs. **6b** & **8a** vs. **8b**) had minor effect on their orientations in the binding site and thus their docking scores. This was rationalized, as the docking studies revealed that hydrophobic sub-pocket **B** is large enough to accommodate bulky substituents offering no additional favorable interaction with the binding site.
- ii. On the contrary, the relative tightness of sub-pocket **A** forms a good platform for molecular design. Introduction of a long

spacer (acetylpiperazinyl) and a large hydrophobic moiety (*o*-methoxyphenyl) in compounds **9a**, **b** resulted in marked improvement of the antiviral activity, reaching  $EC_{50} = 0.79 \mu\text{M}$  for compound **9b**. Exploration of their binding modes in the binding site, revealed binding poses with high docking scores and favorable interactions with the backbone amino acid residues.

#### 5. Experimental

##### 5.1. Chemistry

Melting points were determined with Stuart Scientific apparatus and are uncorrected. FT-IR spectra were recorded on a Perkin–Elmer spectrophotometer and measured by  $\nu'$   $\text{cm}^{-1}$  scale using KBr cell.  $^1\text{H}$  NMR spectra were measured in  $\delta$  scale on a JEOL 300 MHz spectrometer. Unless otherwise stated, the spectra were obtained on solutions in DMSO and referred to TMS. The electron impact (EI) mass spectra were recorded on Finnigan Mat SSQ 7000 (70 eV) mass spectrometer. The peak intensities, in parentheses, are

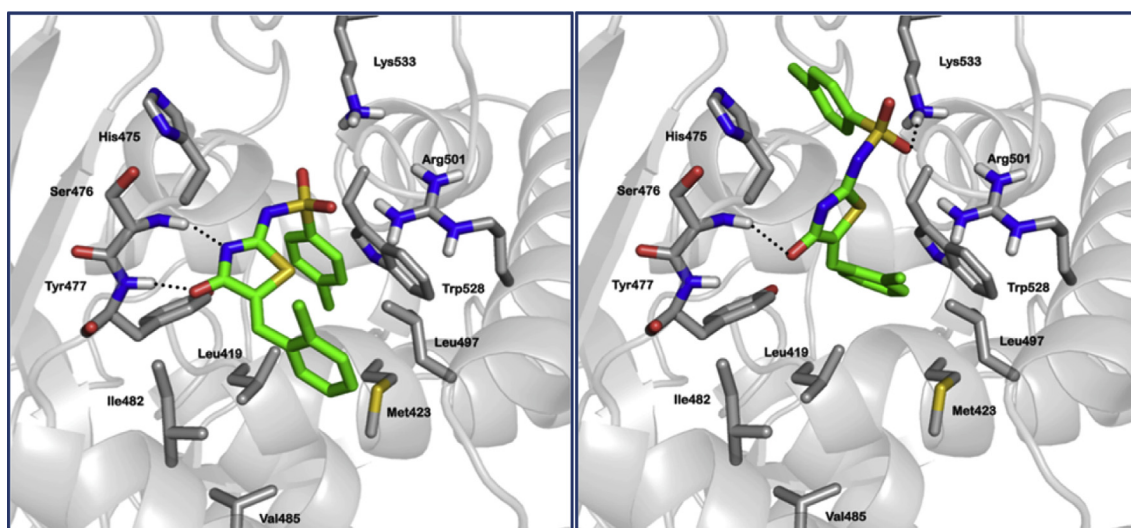


Fig. 3. Two top-ranked docking poses for compound **6g**.

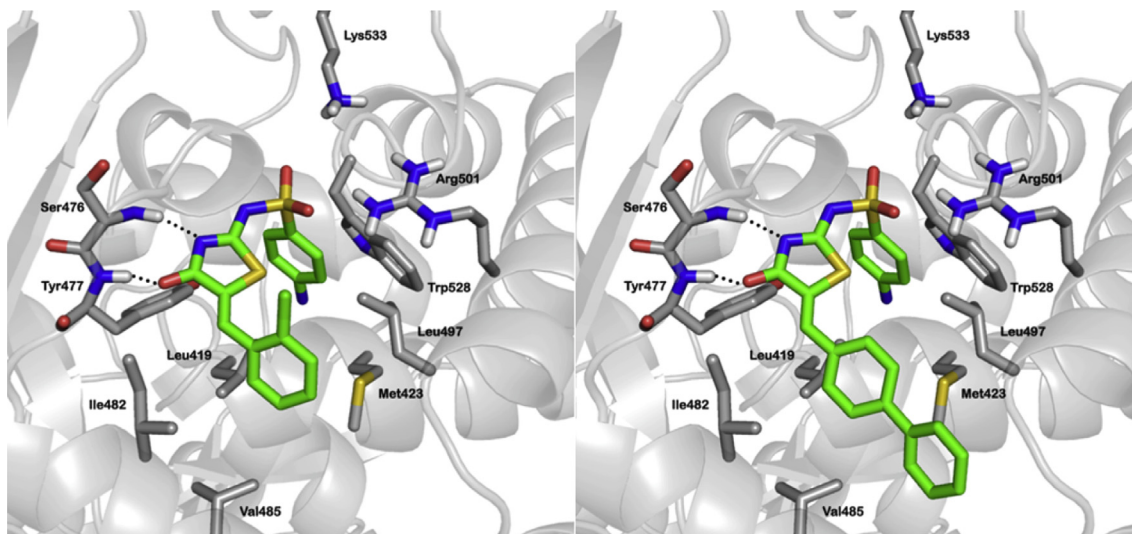


Fig. 4. Top-ranked docking poses for sulfonamides **8a** (left) and **8b** (right).

expressed as percentage abundance. Analytical thin layer chromatography (TLC) was performed on Merck Kieselgel 60PF<sub>254</sub> silica on Aluminum backed sheets. All  $R_f$  values were recorded from the center of the spots. All TLC solvent proportions were measured volume by volume. Column chromatography was performed using Merk Silica gel (mesh size = 0.032–0.064 mm). All reagents and solvents were purified and dried by standard techniques. Solvents were removed under reduced pressure in a rotary evaporator. Elemental microanalysis was performed at the Microanalytical Center, Cairo University; all the values were within range of  $\pm 0.4$ .

#### 5.1.1. 2-Aminothiazol-4(5H)-one (**2**)

Thiourea (7.6 g, 100 mmol) was dissolved in 50 mL 95% ethanol by refluxing for 10–20 min. To the solution, ethylchloroacetate (10.8 mL, 100 mmol) was added slowly through the condenser while gentle reflux was continued. After the mixture had been refluxed for 3 h longer, it was allowed to cool to rt. The formed solid

was filtered by suction on a Buchner funnel and washed with 50 mL ethanol. The crude hydrochloride salt was dissolved in 120 mL of hot, freshly boiled water. A boiling solution of sodium acetate trihydrate (12.1 g, 88 mmol) in 15 mL water was added to the previous solution and the mixture was just heated to boiling. The resulting clear solution was stored in the ice chest overnight. The crystalline pseudothiohydantoin was filtered, washed with water and dried to give **2** as white needle crystals; (9.3 g, 80%); mp 241–243 °C (as reported) [28].

#### 5.1.2. 4-Substituted-benzenesulfonyl chlorides (**3a–c**) [29]

**5.1.2.1. General procedure.** To a solution of chlorosulfonic acid (22.8 mL, 344 mmol) cooled to 0 °C by keeping it in a freezing mixture of ice and salt, the substituted benzene (100 mmol) was introduced dropwise from the dropping funnel at such a rate that the temperature does not exceed 5 °C. When all the substituted benzene has been added (~30 min), the reaction mixture was

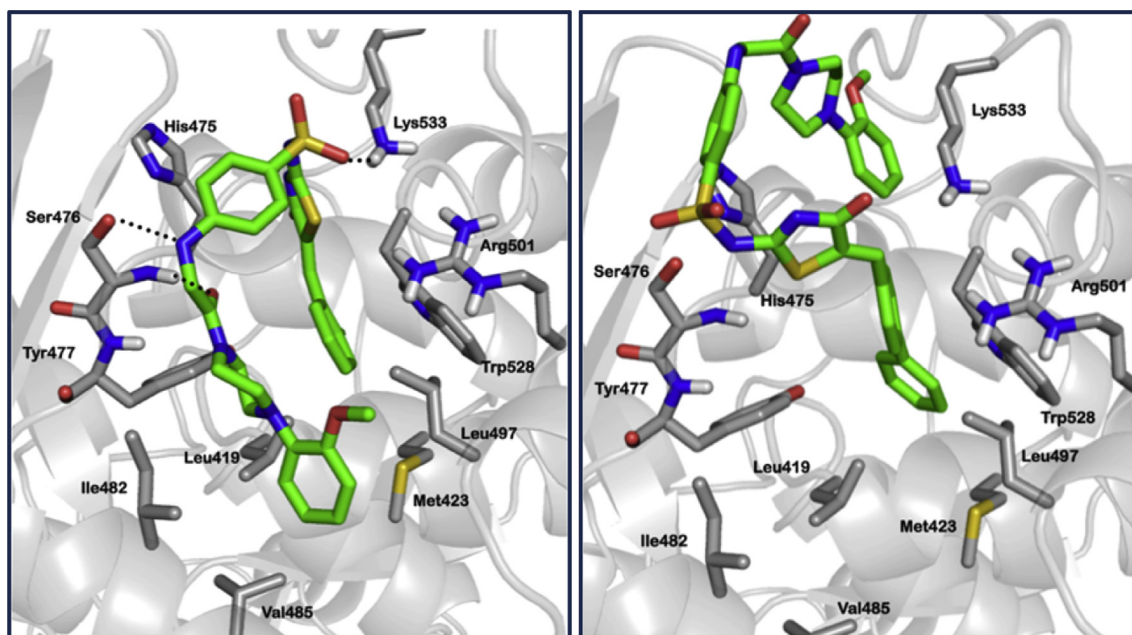
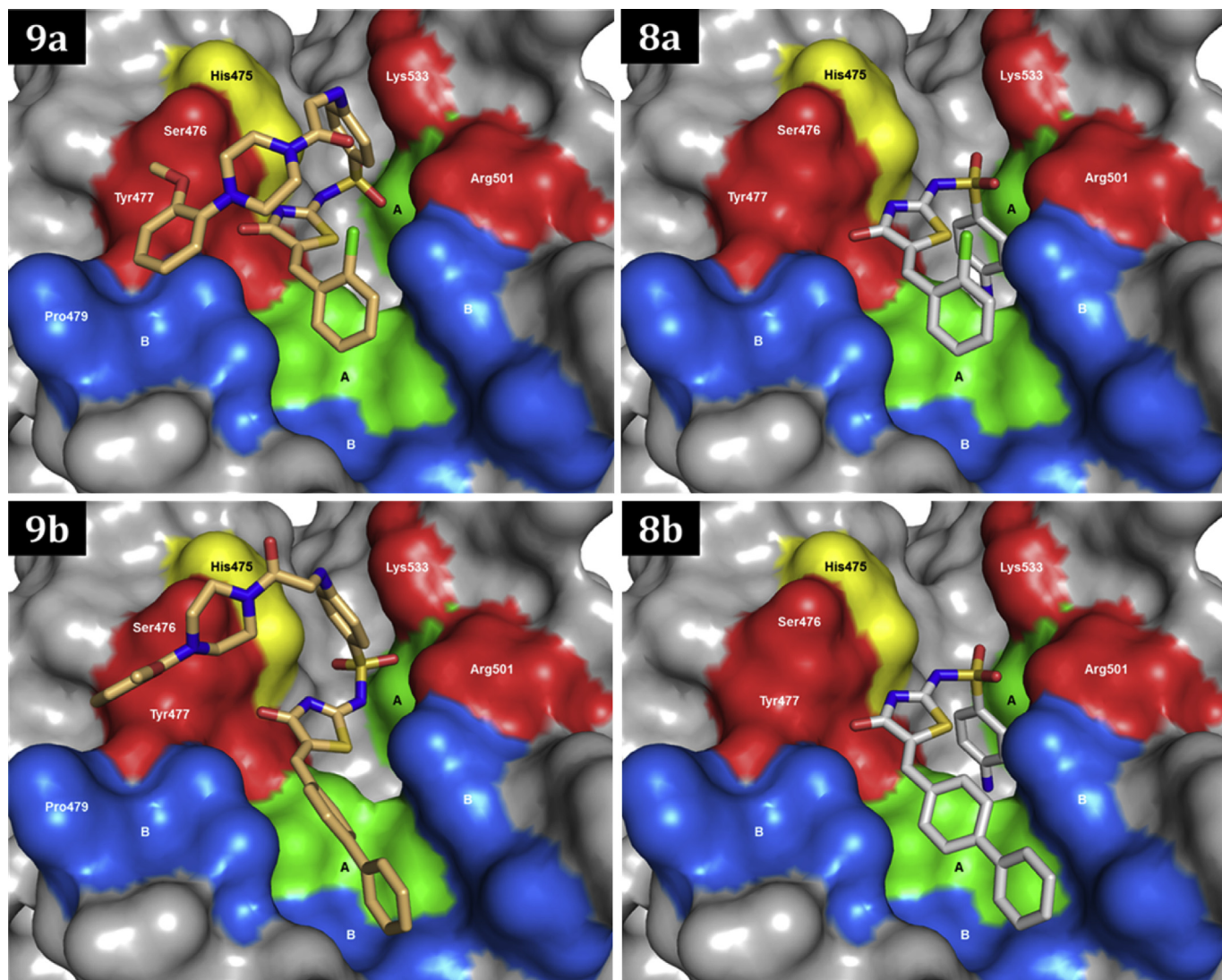


Fig. 5. Top-ranked docking poses for sulfanilamides **9a** (left) and **9b** (right) from rigid-receptor docking.





**Fig. 6.** Semi-automated docking poses for sulfanilamides **9a** and **9b** (orange carbons) in comparison to their unsubstituted amino analogs **8a** and **8b** (white carbons), respectively. Green-surface denotes hydrophobic sub-pockets A (Leu419, Met423 and Trp528) and blue denotes sub-pocket B (Ile482, Val485, Leu489, Pro496 and Leu497). (For interpretation of the references to color in this figure legend, the reader is referred to the web version of this article.)

stirred for 4 h. The reaction mixture was then poured over ice cold water and kept overnight in the refrigerator. The precipitate formed was filtered and washed with water ( $2 \times 10$  mL) to afford the titled products (**3a–c**).

**3a**; mp 69–70 °C (as reported) [30], **3b**; mp 55–57 °C (as reported) [31], **3c**; mp 35–37 °C (as reported) [31].

#### 5.1.3. 4-Substituted-benzenesulfonamidothiazol-4(5H)-ones (**4a–c**)

**5.1.3.1. General procedure.** To a mixture of the corresponding arylsulphonyl chloride (10 mmol) in THF (10 mL) and TEA (3 mL, 30 mmol), **2** (1.16 g, 10 mmol) were added. The reaction mixture was refluxed until the disappearance of the starting material as judged by TLC (~48 h). THF was evaporated under vacuum leaving a solid material which was filtered, washed with water ( $2 \times 10$  mL) and dried over anhydrous calcium chloride to afford the titled products (**4a–c**).

**5.1.3.2. 4-Tolylsulfonamidothiazol-4(5H)-one (4a)** [26]. TLC system ( $\text{CHCl}_3/\text{MeOH}$  8.5:1.5). The product was separated as buff crystals, (1.95 g, 72%); mp 182–184 °C.

**5.1.3.3. 4-Chlorobenzenesulfonamidothiazol-4(5H)-one (4b)** [32]. TLC system ( $\text{CHCl}_3/\text{MeOH}$  9.5:0.5). The product was separated as yellow crystals, (1.85 g, 63%); mp 237–239 °C.

**5.1.3.4. 4-Fluorobenzenesulfonamidothiazol-4(5H)-one (4c)** [32]. TLC system ( $\text{CHCl}_3/\text{MeOH}$  9:1). The product was separated as yellow buff crystals, (1.62 g, 60%); mp > 280 °C.

#### 5.1.4. (Z)-2-Amino-5-(arylmethylene)thiazol-4(5H)-ones (**5a–d**)

**5.1.4.1. General procedure.** A mixture of **2** (1.16 g, 10 mmol), the corresponding aldehyde (10 mmol) and anhydrous sodium acetate (2.40 g, 30 mmol) in glacial acetic acid (15 mL) was refluxed for 16 h. The reaction mixture was allowed to cool to rt, poured onto ice cold water (100 mL) and stirred for 1.5 h. The precipitate was filtered off, washed with water ( $3 \times 10$  mL), then with *n*-hexane ( $2 \times 10$  mL) and dried over anhydrous calcium chloride to afford the titled products (**5a–d**).

**5.1.4.2. (Z)-2-Amino-5-(pyridine-3-ylmethylene)thiazol-4(5H)-one (5a)** [33]. TLC system ( $\text{CHCl}_3/\text{MeOH}$  9.5:0.5). The product was separated as yellow orange crystals, (1.8 g, 76%); mp 284–286 °C.

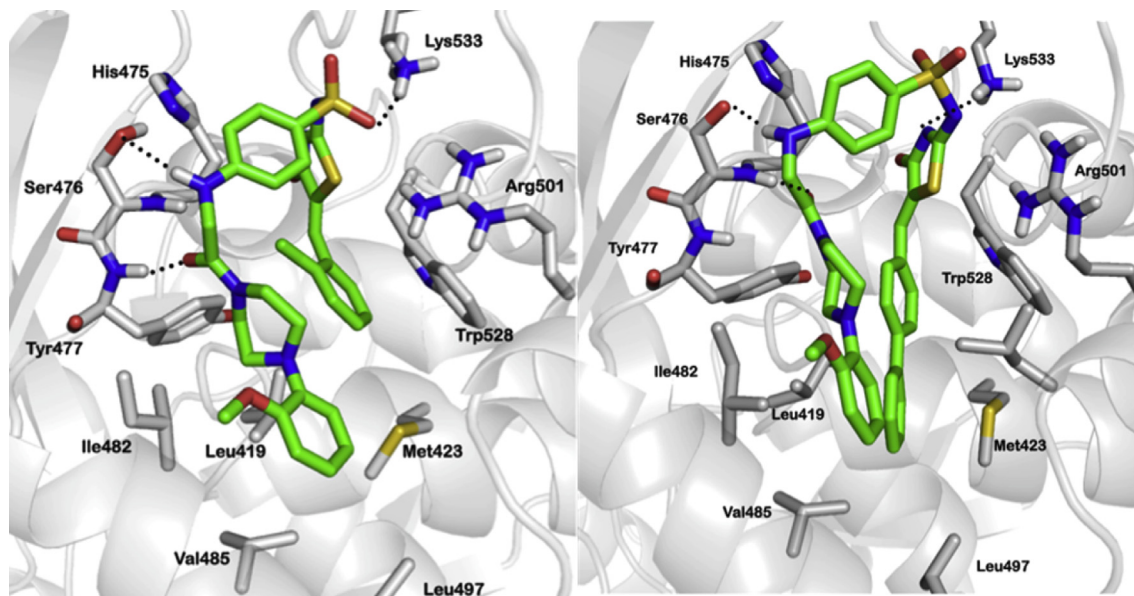


Fig. 7. Top-scored induced-fit docking poses for compounds **9a** (left) and **9b** (right).

5.1.4.3. (*Z*)-2-Amino-5-(4-methoxyphenylmethylene)thiazol-4(5*H*)-one (**5b**). TLC system (CHCl<sub>3</sub>/MeOH 9:1). The product was separated as yellow crystals, (1.82 g, 65%); mp > 300 °C; <sup>1</sup>H NMR (300 MHz, DMSO): δ 9.17 (br, 2H, NH<sub>2</sub>), δ 7.83 (d, 2H, Ar), δ 7.74 (d, 2H, Ar), δ 7.67 (d, 2H, Ar), δ 7.50 (s, 1H, olefin), δ 7.48–7.39 (m, 3H, Ar); FT-IR (ν max, cm<sup>-1</sup>): 3220 (NH<sub>2</sub>), 1670 (C=O); MS (Molecular formula: C<sub>16</sub>H<sub>12</sub>N<sub>2</sub>O<sub>2</sub>S, Mwt.: 280.34): *m/z* 280 (M<sup>+</sup>, 54%), 210 (100%), 165 (15%).

5.1.4.4. (*Z*)-2-Amino-5-(2-chlorophenylmethylene)thiazol-4(5*H*)-one (**5c**) [34]. TLC system (CHCl<sub>3</sub>/MeOH 9:1). The product was separated as yellow buff crystals, (1.48 g, 72%); mp 265–267 °C.

5.1.4.5. (*Z*)-2-Amino-5-(4-biphenylmethylene)thiazol-4(5*H*)-one (**5d**). TLC system (CHCl<sub>3</sub>/MeOH 8:2). The product was separated as yellow crystals, (1.87 g, 80%); mp 272–274 °C; <sup>1</sup>H NMR (300 MHz, DMSO): δ 7.74 (s, 1H, olefin), δ 7.56 (d, *J* = 8.4 Hz, 2H, Ar), δ 7.09 (d, *J* = 8.7 Hz, 2H, Ar), δ 3.71 (s, 3H, –OCH<sub>3</sub>); FT-IR (ν max, cm<sup>-1</sup>): 3340 (NH<sub>2</sub>), 1690 (C=O); MS (Molecular formula: C<sub>11</sub>H<sub>10</sub>N<sub>2</sub>O<sub>2</sub>S, Mwt.: 234.27): *m/z* 234 (M<sup>+</sup>, 23%), 203 (100%), 120 (17%).

5.1.5. (*Z*)-2-Arylsulfonamido-5-(arylmethylene) thiazol-4-(5*H*)-ones (**6a–i**)

5.1.5.1. General procedure

5.1.5.1.1. Method A. A mixture of **4a–c** (10 mmol), the corresponding aldehyde (10 mmol) and anhydrous sodium acetate (2.40 g, 30 mmol) in glacial acetic acid (10 mL) was refluxed for 16 h. The reaction mixture was allowed to cool to rt, poured onto ice cold water (100 mL) and stirred for 1.5 h. The precipitate was filtered off, washed with water (3 × 10 mL), then with n-hexane (2 × 10 mL) and dried over anhydrous calcium chloride. Recrystallization from methanol afforded the titled products (**6a–i**) (64–81%).

5.1.5.2. Method B. To a mixture of the corresponding arylsulphonyl chloride **3a–c** (10 mmol) in THF (10 mL) and TEA (3 mL, 30 mmol), **5a–d** (10 mmol) was added. The reaction mixture was refluxed for 48 h. THF was evaporated under vacuum leaving a solid material which was collected and dissolved in dil. HCl. The mixture was stirred at rt for 1 h to dissolve any unreacted material. The solid precipitate was filtered off, washed with water and dried over anhydrous calcium chloride. Recrystallization from methanol afforded the titled products (**6a–i**) (45–60%).

5.1.5.3. (*Z*)-2-(4-Methylbenzenesulfonamido)-5-(pyridin-3-ylmethylene)thiazol-4-(5*H*)-ones (**6a**). The titled compound was separated as pale yellow crystals (2.62 g, 67%); mp 222–224 °C; <sup>1</sup>H NMR (300 MHz, DMSO): δ 7.89 (s, 1H, olefin), δ 7.73 (d, 2H, Ar), δ 7.62–δ 7.58 (m, 4H, Ar), δ 7.45 (d, 2H, Ar), δ 2.40 (s, 3H, CH<sub>3</sub>); FT-IR

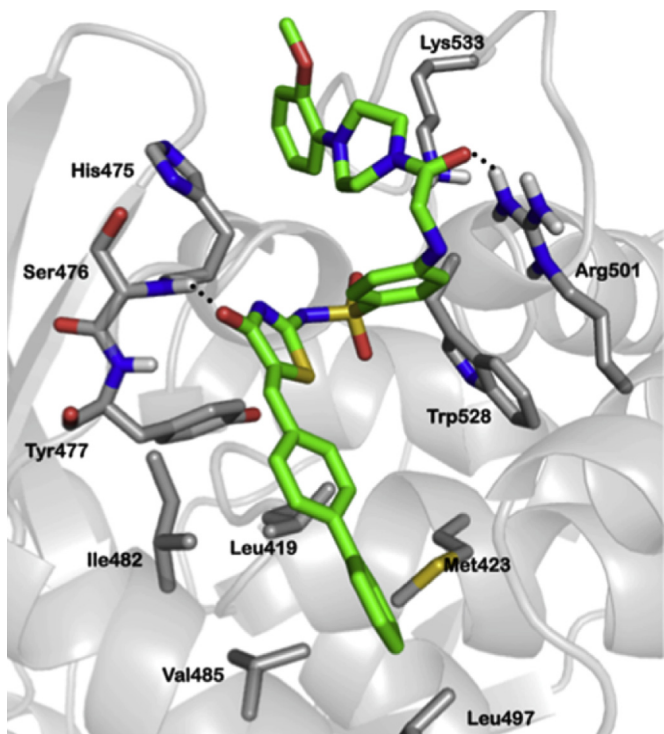


Fig. 8. Lower score induced-fit docking pose for compound **9b** resembles typical co-crystallized ligands.

( $\nu$  max,  $\text{cm}^{-1}$ ): 3120 (NH), 2890 (C–H aliphatic), 1700 (C=O); MS (Mwt.: 392.88):  $m/z$  394 ( $M+2$ , 6.3%), 392 ( $M^+$ , 15%), 168 (100%). Anal. Calcd for  $\text{C}_{17}\text{H}_{13}\text{ClN}_2\text{O}_3\text{S}_2$ : C, 51.97; H, 3.34; N, 7.13; Found: C, 51.62; H, 3.58; N, 6.94.

**5.1.5.4. (Z)-2-(4-Methylbenzenesulfonamido)-5-(4-methoxyphenylmethylene)thiazol-4-(5H)-one (6b).** The titled compound was separated as yellow crystals (3.51 g, 81%); mp > 300 °C;  $^1\text{H}$  NMR (300 MHz, DMSO):  $\delta$  7.91 (d,  $J$  = 7.8 Hz, 2H, Ar),  $\delta$  7.82 (s, 1H, olefin),  $\delta$  7.76 (m, 4H, Ar),  $\delta$  7.51 (m, 3H, Ar),  $\delta$  7.43 (m, 4H, Ar),  $\delta$  2.35 (s, 3H,  $\text{CH}_3$ ); FT-IR ( $\nu$  max,  $\text{cm}^{-1}$ ): 3310 (NH), 2860 (C–H aliphatic), 1670 (C=O); MS (Mwt.: 434.53):  $m/z$  434 ( $M^+$ , 20%), 210 (100%). Anal. Calcd for  $\text{C}_{23}\text{H}_{18}\text{N}_2\text{O}_3\text{S}_2$ : C, 63.57; H, 4.18; N, 6.45; Found: C, 63.22; H, 3.85; N, 6.73.

**5.1.5.5. (Z)-5-(2-Chlorophenylmethylene)-2-(4-methylbenzenesulfonamido)thiazol-4-(5H)-one (6c).** The titled compound was separated as pale yellow crystals (2.51 g, 70%); mp 192–194 °C;  $^1\text{H}$  NMR (300 MHz, DMSO):  $\delta$  10.16 (br, 1H, NH),  $\delta$  8.96 (s, 1H, Ar),  $\delta$  8.72 (d,  $J$  = 5.4 Hz, 1H, Ar),  $\delta$  8.25 (d,  $J$  = 8.7 Hz, 1H, Ar),  $\delta$  7.85 (t,  $J$  = 6.6 Hz, 1H, Ar),  $\delta$  7.68 (s, 1H, olefin),  $\delta$  7.48 (d,  $J$  = 8.1 Hz, 2H, Ar),  $\delta$  7.11 (d,  $J$  = 7.8 Hz, 2H, Ar),  $\delta$  2.28 (s, 3H,  $\text{CH}_3$ ); FT-IR ( $\nu$  max,  $\text{cm}^{-1}$ ): 3400 (NH), 2900 (C–H aliphatic), 1620 (C=O); MS (Mwt.: 359.42):  $m/z$  359 ( $M^+$ , 4%), 205 (67%), 135 (100%). Anal. Calcd for  $\text{C}_{16}\text{H}_{13}\text{N}_3\text{O}_3\text{S}_2$ : C, 53.47; H, 3.65; N, 11.69; Found: C, 53.21; H, 3.93; N, 11.50.

**5.1.5.6. (Z)-5-(4-Biphenylmethylene)-2-(4-methylbenzenesulfonamido)thiazol-4-(5H)-one (6d).** The titled compound was separated as pale yellow crystals (2.87 g, 74%); mp 192–194 °C;  $^1\text{H}$  NMR (300 MHz, DMSO):  $\delta$  9.84 (br, 1H, NH),  $\delta$  7.84 (d,  $J$  = 7.2 Hz, 2H, Ar),  $\delta$  7.71 (s, 1H, olefin),  $\delta$  7.61 (d,  $J$  = 7.2 Hz, 2H, Ar),  $\delta$  7.40 (d,  $J$  = 6.9 Hz, 2H, Ar),  $\delta$  7.12 (d,  $J$  = 8.1 Hz, 2H, Ar),  $\delta$  3.69 (s, 3H,  $-\text{OCH}_3$ ),  $\delta$  2.37 (s, 3H,  $\text{CH}_3$ ); FT-IR ( $\nu$  max,  $\text{cm}^{-1}$ ): 3450 (NH), 2850 (C–H aliphatic), 1680 (C=O); MS (Mwt.: 388.46):  $m/z$  388 ( $M^+$ , 45%), 234 (50%), 164 (100%). Anal. Calcd for  $\text{C}_{18}\text{H}_{16}\text{N}_2\text{O}_4\text{S}_2$ : C, 55.65; H, 4.15; N, 7.21; Found: C, 56.08; H, 4.43; N, 7.56.

**5.1.5.7. (Z)-2-(4-Chlorobenzenesulfonamido)-5-(pyridin-3-ylmethylene)thiazol-4-(5H)-one (6e).** The titled compound was separated as orange crystals (2.42 g, 64%); mp 220–222 °C;  $^1\text{H}$  NMR (300 MHz, DMSO):  $\delta$  8.92 (s, 1H, Ar),  $\delta$  8.69 (d, 1H, Ar),  $\delta$  8.12 (d, 1H, Ar),  $\delta$  7.91 (t, 1H, Ar),  $\delta$  7.83 (s, 1H, olefin),  $\delta$  7.58 (d, 2H, Ar),  $\delta$  7.35 (d, 2H, Ar); FT-IR ( $\nu$  max,  $\text{cm}^{-1}$ ): 3080 (NH), 1690 (C=O); MS (Mwt.: 379.84):  $m/z$  380 ( $M^+$ , 5%), 231 (56%), 174 (83%), 74 (100%). Anal. Calcd for  $\text{C}_{15}\text{H}_{10}\text{ClN}_3\text{O}_3\text{S}_2$ : C, 47.43; H, 2.65; N, 11.06; Found: C, 47.06; H, 2.83; N, 10.78.

**5.1.5.8. (Z)-2-(4-Chlorobenzenesulfonamido)-5-(4-methoxyphenylmethylene)thiazol-4-(5H)-one (6f).** The titled compound was separated as yellow crystals (2.88 g, 72%); mp 176–178 °C;  $^1\text{H}$  NMR (300 MHz, DMSO):  $\delta$  7.90 (d,  $J$  = 8.4 Hz, 2H, Ar),  $\delta$  7.73 (d,  $J$  = 8.7 Hz, 2H, Ar),  $\delta$  7.68 (s, 1H, olefin),  $\delta$  7.54 (d,  $J$  = 8.4 Hz, 2H, Ar),  $\delta$  7.11 (d,  $J$  = 8.7 Hz, 2H, Ar),  $\delta$  3.84 (s, 3H,  $-\text{OCH}_3$ ); FT-IR ( $\nu$  max,  $\text{cm}^{-1}$ ): 3220 (NH), 2800 (C–H aliphatic), 1710 (C=O); MS (Mwt.: 408.88):  $m/z$  408 ( $M^+$ , 2%), 231 (26%), 148 (100%). Anal. Calcd for  $\text{C}_{17}\text{H}_{13}\text{ClN}_2\text{O}_4\text{S}_2$ : C, 49.94; H, 3.20; N, 6.85; Found: C, 49.62; H, 3.11; N, 7.24.

**5.1.5.9. (Z)-2-(4-Chlorobenzenesulfonamido)-5-(2-chlorophenylmethylene)thiazol-4-(5H)-one (6g).** The titled compound was separated as white crystals (3.34 g, 81%); mp 195–197 °C;  $^1\text{H}$  NMR (300 MHz, DMSO):  $\delta$  9.58 (br, 1H, NH),  $\delta$  7.90 (d,  $J$  = 8.7 Hz, 2H, Ar),  $\delta$  7.78 (s, 1H, olefin),  $\delta$  7.68 (d,  $J$  = 8.7 Hz, 2H, Ar),  $\delta$  7.48 (m, 4H, Ar); FT-IR ( $\nu$  max,  $\text{cm}^{-1}$ ): 3240 (NH), 1680 (C=O); MS (Mwt.: 413.3):  $m/z$  413 ( $M^+$ , 3%), 202 (35%), 174 (7%), 167 (100%). Anal. Calcd for

$\text{C}_{16}\text{H}_{10}\text{Cl}_2\text{N}_2\text{O}_3\text{S}_2$ : C, 46.50; H, 2.44; N, 6.78; Found: C, 46.78; H, 2.65; N, 7.13.

**5.1.5.10. (Z)-2-(4-Fluorobenzenesulfonamido)-5-(4-methoxyphenylmethylene)thiazol-4-(5H)-one (6h).** The titled compound was separated as bright yellow crystals (2.51 g, 65%); mp 243–245 °C;  $^1\text{H}$  NMR (300 MHz, DMSO):  $\delta$  7.98 (m, 2H, Ar),  $\delta$  7.75 (s, 1H, olefin),  $\delta$  7.63 (d,  $J$  = 8.7 Hz, 2H, Ar),  $\delta$  7.46 (t,  $J$  = 8.8 Hz, 2H, Ar),  $\delta$  7.09 (d,  $J$  = 8.7 Hz, 2H, Ar),  $\delta$  3.84 (s, 3H,  $-\text{OCH}_3$ ); FT-IR ( $\nu$  max,  $\text{cm}^{-1}$ ): 3100 (NH), 2900 (C–H aliphatic), 1720 (C=O); MS (Mwt.: 392.42):  $m/z$  392 ( $M^+$ , 2%), 235 (50%), 164 (100%). Anal. Calcd for  $\text{C}_{17}\text{H}_{13}\text{FN}_2\text{O}_4\text{S}_2$ : C, 52.03; H, 3.34; N, 7.14; Found: C, 51.84; H, 3.21; N, 7.46.

**5.1.5.11. (Z)-2-(4-Fluorobenzenesulfonamido)-5-(2-chlorophenylmethylene)thiazol-4-(5H)-one (6i).** The titled compound was separated as buff crystals (2.96 g, 75%); mp 272–274 °C;  $^1\text{H}$  NMR (300 MHz, DMSO):  $\delta$  9.25 (br, 1H, NH),  $\delta$  7.97–7.61 (m, 4H, Ar),  $\delta$  7.58 (s, 1H, olefin),  $\delta$  7.56–7.45 (m, 4H, Ar); FT-IR ( $\nu$  max,  $\text{cm}^{-1}$ ): 3120 (NH), 1730 (C=O); MS (Mwt.: 396.84):  $m/z$  398 ( $M+2$ , 5%), 396 (12%), 203 (36%), 170 (43%), 168 (100%). Anal. Calcd for  $\text{C}_{16}\text{H}_{10}\text{ClFN}_2\text{O}_3\text{S}_2$ : C, 48.42; H, 2.54; N, 7.06; Found: C, 48.13; H, 2.87; N, 7.39.

#### 5.1.6. (Z)-4-Acetamidophenylsulfonamido-5-(arylmethylene)thiazol-4(5H)-one (7a, b)

**5.1.6.1. General procedure.** To a mixture of the corresponding 4-acetamidobenzenesulphonyl chloride (2.32 g, 10 mmol) in THF (10 mL) and TEA (3 mL, 30 mmol), **5c, d** (10 mmol) was added. The reaction mixture was refluxed for 24 h. THF was evaporated under vacuum leaving a solid material which was collected and dissolved in dil. HCl. The mixture was stirred at rt for 10 h to dissolve any unreacted material. The solid precipitate was filtered off, washed with water and dried over anhydrous calcium chloride. Recrystallization from methanol afforded the titled products (**7a, b**).

**5.1.6.2. (Z)-4-Acetamidophenylsulfonamido-5-(2-chlorophenylmethylene)thiazol-4(5H)-one (7a).** TLC system ( $\text{CHCl}_3/\text{MeOH}$  9.5:0.5). The product was separated as white crystals, (2.95 g, 68%); mp > 280 °C.

**5.1.6.3. (Z)-4-Acetamidophenylsulfonamido-5-(4-biphenylmethylene)thiazol-4(5H)-one (7b).** TLC system ( $\text{CHCl}_3/\text{MeOH}$  9.5:0.5). The product was separated as white crystals, (2.96 g, 62%); mp > 280 °C.

#### 5.1.7. (Z)-4-Aminophenylsulfonamido-5-(arylmethylene)thiazol-4(5H)-ones (8a, b)

**5.1.7.1. General procedure.** The respective **7a, b** (10 mmol) was refluxed in 2 N HCl (20 mL) for 2 h. The reaction mixture was left to cool then filtered to get rid of any unreacted material.  $\text{Na}_2\text{CO}_3$  was added to the filtrate until effervescence stopped. Herein, the crude product precipitated. The mixture was kept in the refrigerator overnight, then it was filtered, the residue washed with water (2  $\times$  10 mL) and dried over anhydrous calcium chloride. Recrystallization from ether afforded the titled products **8a, b**.

**5.1.7.2. (Z)-4-Aminophenylsulfonamido-5-(2-chlorophenylmethylene)thiazol-4(5H)-one (8a).** The titled compound was separated as orange crystals (2.82 g, 72%); mp 180–182 °C;  $^1\text{H}$  NMR (300 MHz, DMSO):  $\delta$  12.73 (br, 2H,  $-\text{NH}_2$ ),  $\delta$  7.92 (s, 1H, olefin),  $\delta$  7.64 (d, 2H, Ar),  $\delta$  7.55 (d, 2H, Ar),  $\delta$  7.52–7.47 (m, 4H, Ar); FT-IR ( $\nu$  max,  $\text{cm}^{-1}$ ): 3280 ( $\text{NH}_2$ ), 1690 (C=O); MS (Molecular formula:  $\text{C}_{16}\text{H}_{12}\text{ClN}_3\text{O}_3\text{S}_2$ , Mwt.: 393.87):  $m/z$  394 ( $M^+$ , 6%), 204 (51%), 168 (100%).

**5.1.7.3. (Z)-4-Aminophenylsulfonamido-5-(4-biphenylmethylene)thiazol-4(5H)-one (8b).** The titled compound was separated as pale



yellow crystals (2.91 g, 67%); mp > 300 °C;  $^1\text{H}$  NMR (300 MHz, DMSO):  $\delta$  9.42 (br, 2H,  $-\text{NH}_2$ ),  $\delta$  9.17 (s, 1H,  $-\text{NH}-\text{SO}_2$ ),  $\delta$  7.84 (s, 1H, olefin),  $\delta$  7.82–7.75 (m, 5H, Ar),  $\delta$  7.65–7.60 (m, 4H, Ar),  $\delta$  7.47–7.42 (m, 4H, Ar), FT-IR ( $\nu$  max,  $\text{cm}^{-1}$ ): 3120 ( $\text{NH}_2$ ), 1670 ( $\text{C}=\text{O}$ ); MS (Molecular formula:  $\text{C}_{22}\text{H}_{17}\text{N}_3\text{O}_3\text{S}_2$ , Mwt.: 435.52):  $m/z$  435 ( $\text{M}^+$ , 2%), 280 (15%), 210 (100%).

**5.1.8. (Z)-N-(5-Arylmethylene-4-oxo-4,5-dihydrothiazol-2-yl)-4-{2-[4-(2-methoxyphenyl)piperazin-1-yl]-2-oxoethylamino} benzenesulfonamides (**9a, b**)**

**5.1.8.1. General procedure.** To a mixture of the respective (**8a, b**) (10 mmol) and  $\text{K}_2\text{CO}_3$  (2.96 g, 20 mmol) in dry acetone (10 mL), 1-(2-chloroacetyl)-4-(2-methoxyphenyl)piperazine (2.68 g, 10 mmol) was added. The reaction mixture was refluxed for 24 h, left to cool and then filtered. The filtrate was evaporated under vacuum. The crude product was washed with water ( $2 \times 10$  mL) and dried over anhydrous calcium chloride. Recrystallization from ether afforded the titled compounds (**9a, b**).

**5.1.8.2. (Z)-N-[5-(2-Chlorobenzylidene)-4-oxo-4,5-dihydrothiazol-2-yl]-4-{2-[4-(2-methoxyphenyl)piperazin-1-yl]-2-oxoethylamino} benzenesulfonamide (**9a**).** The titled compound was separated as bright yellow crystals (4.25 g, 68%); mp 210–212 °C;  $^1\text{H}$  NMR (300 MHz, DMSO):  $\delta$  7.72 (s, 1H, olefin),  $\delta$  7.62–7.29 (m, 7H, Ar),  $\delta$  6.93–6.88 (m, 5H, Ar),  $\delta$  4.66 (s, 2H,  $-\text{CH}_2-\text{CO}-$ ),  $\delta$  3.77 (s, 3H,  $-\text{OCH}_3$ ), 3.61–3.55 (m, 4H, piperazine), 3.05–2.91 (m, 4H, piperazine), FT-IR ( $\nu$  max,  $\text{cm}^{-1}$ ): 3310 (NH), 2870 (C–H aliphatic), 1670 ( $\text{C}=\text{O}$ ); MS (Mwt.: 626.15):  $m/z$  626 ( $\text{M}^+$ , 3%), 470 (4%), 280 (15%), 210 (100%). Anal. Calcd for  $\text{C}_{29}\text{H}_{28}\text{ClN}_5\text{O}_5\text{S}_2$ : C, 55.63; H, 4.51; N, 11.18; Found: C, 56.07; H, 4.25; N, 10.83.

**5.1.8.3. (Z)-N-[5-(Biphenyl-4-ylmethylene)-4-oxo-4,5-dihydrothiazol-2-yl]-4-{2-[4-(2-methoxyphenyl)piperazin-1-yl]-2-oxoethylamino} benzenesulfonamide (**9b**).** The titled compound was separated as buff crystals (3.86 g, 58%); mp 232–234 °C;  $^1\text{H}$  NMR (300 MHz, DMSO):  $\delta$  7.84 (s, 1H, olefin),  $\delta$  7.82–7.73 (m, 5H, Ar),  $\delta$  7.68–7.64 (m, 4H, Ar),  $\delta$  7.49–7.41 (m, 4H, Ar),  $\delta$  6.96–6.91 (m, 4H, Ar),  $\delta$  4.69 (s, 2H,  $-\text{CH}_2-\text{CO}-$ ),  $\delta$  3.79 (s, 3H,  $-\text{OCH}_3$ ), 3.68–3.50 (m, 4H, piperazine), 3.02–2.93 (m, 4H, piperazine), FT-IR ( $\nu$  max,  $\text{cm}^{-1}$ ): 3100 (NH), 2920 (C–H aliphatic), 1710 ( $\text{C}=\text{O}$ ); MS (Mwt.: 667.80):  $m/z$  667 ( $\text{M}^+$ , 6%), 514 (3%), 280 (23%), 210 (100%). Anal. Calcd for  $\text{C}_{35}\text{H}_{33}\text{N}_5\text{O}_5\text{S}_2$ : C, 62.95; H, 4.98; N, 10.49; Found: C, 62.67; H, 5.20; N, 10.78.

## 5.2. Biological evaluation

Biological evaluation studies were performed at the Rega institute, Katholique university of Leuven, Faculty of Medicine, Belgium.

### 5.2.1. Cell culture and dose-response assays

One day before addition of the test compounds, Human hepatoma cells (Huh5.2) containing the hepatitis C virus genotype 1b 1389luc-ubi-neo/NS3-3'/5.1 replicon were sub-cultured in Dulbecco's modified Eagle medium (DMEM) (Cat. N° 41965039) supplemented with 10% fetal calf serum (FCS), 1% non-essential amino acids (11140035), 1% penicillin/streptomycin (15140148) and 2% Geneticin (10131027); Invitrogen. Cell lines were grown for 3–4 days in 75  $\text{cm}^2$  tissue culture flasks (Techno Plastic Products), harvested and seeded in assay medium (DMEM, 10% FCS, 1% non-essential amino acids, 1% penicillin/streptomycin) at a density of 6500 cells/well (100  $\mu\text{L}$ /well) in 96-well tissue culture microtiter plates (Falcon, Beckton Dickinson for evaluation of anti-metabolic effect and Culture Plate, Perkin Elmer for evaluation of antiviral effect). The microtiter plates were incubated overnight (37 °C, 5%  $\text{CO}_2$ , 95–99% relative humidity), yielding a non-confluent cell monolayer.

The evaluations of the anti-metabolic as well as the antiviral effect of each compound were performed in parallel. Four-step, 1-to-5 test compound dilution series were prepared. Following assay setup, the microtiter plates were incubated for 72 h (37 °C, 5%  $\text{CO}_2$ , 95–99% relative humidity).

### 5.2.2. Assay protocols

**5.2.2.1. Luciferase assay.** For the evaluation of antiviral effects, viral RNA replication was determined using Firefly luciferase assay. Assay medium was aspirated and the cell monolayers were washed with PBS (phosphate-buffered saline). The wash buffer was aspirated, 25  $\mu\text{L}$  of GloLysis Buffer (Cat. N°. E2661, Promega) was added after which lysis was allowed to proceed for 5 min at rt. Subsequently, 50  $\mu\text{L}$  of Luciferase Assay System (Cat. N°. E1501, Promega) was added and the luciferase luminescence signal was quantified immediately (1000 ms integration time/well, Safire<sup>2</sup>, Tecan). Relative luminescence units were converted to percentage of untreated controls.

**5.2.2.2. Viability assay.** For the evaluation of the anti-metabolic effects, the assay medium was aspirated, replaced with 75  $\mu\text{L}$  of a 5% MTS (Promega) solution in phenol red-free medium and incubated for 1.5 h (37 °C, 5%  $\text{CO}_2$ , 95–99% relative humidity). Absorbance was measured at a wavelength of 498 nm (Safire<sup>2</sup>, Tecan) and optical densities (OD values) were converted to percentage of untreated controls.

## 5.3. Molecular modeling

### 5.3.1. Building ligands

All studied ligands were constructed as 2D structures on ChemBioDraw Ultra and converted into corresponding SMILES strings, from which 3D structures were generated using openbabel [35]. The 3D structures were imported into Maestro [36] and were subjected to geometry optimization using MacroModel [37] employing OPLS-AA 2005 force field with GB/SA solvent continuum model [38] as potential function. Minimization converged to threshold gradient of 0.0001 kJ/mol Å. Protonation states for both sulfonamides and carboxylate compounds were assigned by Epik [39]. Sulfonamides exhibited higher predicted pKa values (5.5–7.0) compared to their carboxylate analogs (~2.0), and hence they were modeled in their neutral form, while carboxylates were modeled as the negatively ionized species.

### 5.3.2. Preparing enzyme structures

Complexes of HCV NS5B polymerase with various ligands were downloaded from the Protein Data Bank. For each crystal structure hydrogens were added, water molecules were removed and bond orders for proteins and ligand were corrected using Maestro Protein Preparation Wizard. Prime [40] was used to fill in missing residues (e.g. residues 149–153 and 565–570 in 2HWH). Partial charges were calculated from OPLS\_2005 force field while protonation states and oxidation states for metals were assigned by Epik [39]. Orientations of added hydrogens were extensively sampled for optimal H-bond formation and the model was then refined by minimization to RMSD threshold of 0.3 Å.

### 5.3.3. Automated Glide docking

For the purpose of docking ligands to protein active sites, the molecular docking program Glide (Grid-based Ligand Docking with Energetics) [41] was used in this study. Crystal structure of HCV NS5B polymerase with the carboxylate derivative **2** was used for docking grid generation (PDB: 2HWH, resolution 2.0 Å). Terminal hydroxyl groups of binding site serine, threonine and tyrosine residues were treated as 'rotatable groups' within the generated



grid. Number of poses allowed to pass through the initial Glide screens was increased from the default 5000 to 50,000. The energy window for keeping initial poses was set to 100.0 kcal/mol and the best 1000 poses for each ligand were kept for energy minimization. Finally, atoms with partial charges <0.15 were scaled down in size by a factor of 0.8 to soften the potential for non-polar parts of the ligand. Output for each ligand included a maximum of 10 *distinct* poses.

Since compounds **9a** and **9b** are relatively bigger in size and hence some degree of receptor re-adjustment might be necessary to accommodate them in the binding site of NS5B polymerase, induced-fit docking of Schrödinger Suite was applied. The induced-fit docking methodology combines Glide and Prime technologies [42]. After initial Glide docking, amino acids within 5.0 Å radius around any suggested pose were considered as flexible, and their side chain conformations were optimized by Prime. Up to 50 poses were retained for each calculation within an energy window of 40.0 kcal/mol to allow for larger diversity in output poses. Poses were finally energy minimized, re-scored, and prioritized by Glide SP scoring. Glide calculates per-residue interaction energies as the sum of OPLS\_2005 non-bonded terms (van der Waals, Columbic and H-bond terms) for all residues within 12.0 Å distance from any found pose. Interactions fingerprints were calculated for studied compounds by summing per-residue interaction energies for amino acids comprising the NS5B polymerase allosteric thumb II polar sub-site (Ser476 + Tyr477 + Arg501 + Lys533), hydrophobic sub-site A (Leu419 + Met423 + Trp528), and hydrophobic sub-site B (Ile482 + Val485 + Leu489 + Pro496 + Leu497). Interaction fingerprints for studied compounds are given in Table 3.

## Acknowledgments

The authors are grateful to Dr. Pieter Leyssen at Laboratory for Virology and Experimental Chemotherapy, Rega Institute for Medical Research (KU Leuven), Leuven, Belgium for performing the virus-cell-based assay.

## Appendix A. Supplementary data

Supplementary data related to this article can be found at <http://dx.doi.org/10.1016/j.ejmech.2013.07.006>.

## References

- [1] J. Alter Miriam, Epidemiology of hepatitis C virus infection, *World Journal of Gastroenterology*: WJG 13 (2007) 2436–2441.
- [2] W. Shepard Colin, L. Finelli, J. Alter Miriam, Global epidemiology of hepatitis C virus infection, *The Lancet Infectious Diseases* 5 (2005) 558–567.
- [3] S. Naggie, K. Patel, J. McHutchison, Hepatitis C virus directly acting antivirals: current developments with NS3/4A HCV serine protease inhibitors, *Journal of Antimicrobial Chemotherapy* 65 (2010) 2063–2069.
- [4] S. Jones, Techniques and applications: breakthrough for HCV research, *Nature Reviews Microbiology* 3 (2005) 585.
- [5] K. Okamoto, M. Mandai, K. Mimura, Y. Murawaki, I. Yuasa, The association of MMP-1, -3 and -9 genotypes with the prognosis of HCV-related hepatocellular carcinoma patients, *Research Communications in Molecular Pathology and Pharmacology* 117–118 (2005) 77–89.
- [6] Anonymous, National Institutes of Health Consensus Development Conference Statement: management of hepatitis C: 2002–June 10–12, 2002, *Hepatology* (Baltimore, Md.) 36 (2002) S21–S29.
- [7] H. Hoofnagle Jay, Course and outcome of hepatitis C, *Hepatology* (Baltimore, Md.) 36 (2002) S21–S29.
- [8] J. Cohen, The scientific challenge of hepatitis C, *Science* (Washington, DC) 285 (1999) 26–30.
- [9] Anonymous, National Institutes of Health Consensus Development Conference Statement: management of hepatitis C 2002 (June 10–12, 2002), *Gastroenterology* 123 (2002) 2082–2099.
- [10] Anonymous, Global surveillance and control of hepatitis C. Report of a WHO Consultation organized in collaboration with the Viral Hepatitis Prevention Board, Antwerp, Belgium, *Journal of Viral Hepatitis* 6 (1999) 35–47.
- [11] M. Willems, H.J. Metselaar, H.W. Tilanus, S.W. Schalm, R.A. De Man, Liver transplantation and hepatitis C, *Transplant International* 15 (2002) 61–72.
- [12] G.W. McCaughan, M. Omata, D. Amarapurkar, S. Bowden, W.C. Chow, A. Chutaputti, G. Dore, E. Gane, R. Guan, S.S. Hamid, W. Hardikar, C.K. Hui, W. Jafri, J.D. Jia, M.Y. Lai, L. Wei, N. Leung, T. Piratvisuth, S. Sarin, J. Sollano, R. Tateishi, Asian Pacific Association for the Study of the Liver consensus statements on the diagnosis, management and treatment of hepatitis C virus infection, *Journal of Gastroenterology and Hepatology* 22 (2007) 615–633.
- [13] E. Jaeckel, M. Cornberg, H. Wedemeyer, T. Santantonio, J. Mayer, M. Zankel, G. Pastore, M. Dietrich, C. Trautwein, M.P. Manns, B. Atzler, S. Walker, G. Berger, A. Bieberle, D. Schoett, J. Bubeck, P. Buggisch, H. Greten, C.R. de Mas, T. Bozkurt, J. Eichmueller, W.P. Fritsch, C. Gerasch, P. Halberstadt, J. Epping, H. Hinrichsen, U.R. Foelsch, J. Kemper, F. Kozel, W. Kraupa, T. Schneider, M.R. Kraus, K. Wilms, J. Kroeger, M. Zeitz, P. Leidig, D. Leykam, R. Linhart, U. Lippert, V. Makelke, K. Mohsen, K. Pries, B. Pusch, H. Lutz, R.D. Rackwitz, R. Goetz, M. Respondek, W. Zoller, A. Schober, A. Schramm, M. Schwerdtfeger, W.E. Flegg, A. Steinmetz, U. Tiwisina, U. Treichel, G. Gerken, J. Hadem, S. Heringlake, N. Koerbel, T. Mansuroglu, A. Schneider, A. Schueler, J. Wedemeyer, Treatment of acute hepatitis C with interferon  $\alpha$ -2b, *New England Journal of Medicine* 345 (2001) 1452–1457.
- [14] T. Santantonio, M. Fasano, E. Sinisi, A. Guastadisegni, C. Casalino, M. Mazzola, R. Francavilla, G. Pastore, Efficacy of a 24-week course of PEG-interferon  $\alpha$ -2b monotherapy in patients with acute hepatitis C after failure of spontaneous clearance, *Journal of Hepatology* 42 (2005) 329–333.
- [15] T. Shimakami, R.E. Lanford, S.M. Lemon, Hepatitis C: recent successes and continuing challenges in the development of improved treatment modalities, *Current Opinion in Pharmacology* 9 (2009) 537–544.
- [16] T. Oze, N. Hiramatsu, T. Yakushiji, K. Mochizuki, M. Oshita, H. Hagiwara, E. Mita, T. Ito, H. Fukui, Y. Inui, T. Hijioka, M. Inada, K. Kayayama, S. Tamura, H. Yoshihara, A. Inoue, Y. Imai, M. Kato, T. Miyagi, Y. Yoshida, T. Tatsumi, S. Kiso, T. Kanto, A. Kasahara, T. Takehara, N. Hayashi, Indications and limitations for aged patients with chronic hepatitis C in pegylated interferon  $\alpha$ -2b plus ribavirin combination therapy, *Journal of Hepatology* 54 (2011) 604–611.
- [17] S. Munir, S. Saleem, M. Idrees, A. Tariq, S. Butt, B. Rauff, A. Hussain, S. Badar, M. Naudhani, Z. Fatima, M. Ali, L. Ali, M. Akram, M. Aftab, B. Khubaib, Z. Awan, Hepatitis C treatment: current and future perspectives, *Virology Journal* 7 (2010) 296.
- [18] K.J. Lee, J. Choi, J.-h. Ou, M.M.C. Lai, The C-terminal transmembrane domain of hepatitis C virus (HCV) RNA polymerase is essential for HCV replication in vivo, *Journal of Virology* 78 (2004) 3797–3802.
- [19] J.Z. Wu, Z. Hong, Targeting NS5B RNA-dependent RNA polymerase for anti-HCV chemotherapy, *Current Drug Targets: Infectious Disorders* 3 (2003) 207–219.
- [20] L.J. Stuyver, T.R. McBrayer, P.M. Tharnish, J. Clark, L. Hollecker, S. Lostia, T. Nachman, J. Grier, M.A. Bennett, M.-Y. Xie, R.F. Schinazi, J.D. Morrey, J.L. Julander, P.A. Furman, M.J. Otto, Inhibition of hepatitis C replicon RNA synthesis by  $\beta$ -D-2'-deoxy-2'-fluoro-2'-C-methylcytidine: a specific inhibitor of hepatitis C virus replication, *Antiviral Chemistry & Chemotherapy* 17 (2006) 79–87.
- [21] D.M. Jensen, A. Ascione, Future directions in therapy for chronic hepatitis C, *Antiviral Therapy* 13 (2008) 31–36.
- [22] M.J. Sofia, W. Chang, P.A. Furman, R.T. Mosley, B.S. Ross, Nucleoside, nucleotide and non-nucleoside inhibitors of hepatitis C virus NS5B RNA-dependent RNA-polymerase, *Journal of Medicinal Chemistry* 55 (2012) 2481–2531.
- [23] S. Chinnaswamy, H. Cai, C. Kao, An update on small molecule inhibitors of the HCV NS5B polymerase: effects on RNA synthesis in vitro and in cultured cells, and potential resistance in viral quasispecies, *Virus Adaptation and Treatment* 2 (2010) 73–89.
- [24] S. Yan, T. Appleby, G. Larson, J.Z. Wu, R. Hamatake, Z. Hong, N. Yao, Structure-based design of a novel thiazolone scaffold as HCV NS5B polymerase allosteric inhibitors, *Bioorganic & Medicinal Chemistry Letters* 16 (2006) 5888–5891.
- [25] S. Yan, T. Appleby, G. Larson, J.Z. Wu, R.K. Hamatake, Z. Hong, N. Yao, Thiazolone-acylsulfonamides as novel HCV NS5B polymerase allosteric inhibitors: convergence of structure-based drug design and X-ray crystallographic study, *Bioorganic & Medicinal Chemistry Letters* 17 (2007) 1991–1995.
- [26] Y. Ding, K.L. Smith, C.V.N.S. Varaprasad, E. Chang, J. Alexander, N. Yao, Synthesis of thiazolone-based sulfonamides as inhibitors of HCV NS5B polymerase, *Bioorganic & Medicinal Chemistry Letters* 17 (2007) 841–845.
- [27] S. Yan, G. Larson, J.Z. Wu, T. Appleby, Y. Ding, R. Hamatake, Z. Hong, N. Yao, Novel thiazolones as HCV NS5B polymerase allosteric inhibitors: further designs, SAR, and X-ray complex structure, *Bioorganic & Medicinal Chemistry Letters* 17 (2007) 63–67.
- [28] C.F.H. Allen, J.A. VanAllan, Pseudothiohydantoin, *Organic Syntheses* 27 (1947) 6–17.
- [29] E.H. Huntress, F.H. Carten, Identification of organic compounds. I. Chlorosulfonic acid as a reagent for the identification of aryl halides, *Journal of the American Chemical Society* 62 (1940) 511–514.
- [30] J.E. Nordlander, W.J. Kelly, Partial acetylation of neopentyl tosylate-sulfonyl-oxygen-18. An attempt to trap neopentyl cation, *Journal of Organic Chemistry* 32 (1967) 4122–4124.
- [31] Y. Yoshii, A. Ito, T. Hirashima, S. Shinkai, O. Manabe, A kinetic study of the Friedel-Crafts reaction of naphthalene with p-substituted benzenesulfonyl chlorides; the effect of the substituent, *Journal of the Chemical Society, Perkin Transactions 2: Physical Organic Chemistry* (1972–1999) (1988) 777–781.

- [32] M.E. Hultquist, R.P. Germann, J.S. Webb, W.B. Wright Jr., B. Roth, J.M. Smith Jr., Y. SubbaRow, *N*-Heterocyclic benzenesulfonamides, *Journal of the American Chemical Society* 73 (1951) 2558–2566.
- [33] M.T. Omar, F.A. Sherif, Studies on 4-thiazolidinones. VI. Reactions of 5-(aryl-methylene)-2-(alkylthio)-2-thiazolin-4-ones with ammonium carbonate and amines, *Journal Für Praktische Chemie (Leipzig)* 322 (1980) 835–842.
- [34] L. Yu, Q. Dong, F. Pierre, E. Chang, H. Lang, Y. Qjin, Y. Fang, M. Hansen, M. Pellicchia, Common Ligand Mimics: Thiazolidinediones and Rhodanines, *US Patent App.* 10/081,989, USA, 2004, p. 110.
- [35] The Open Babel Package, Version 2.0.1, <http://openbabel.sourceforge.net/>.
- [36] Maestro, Version 9.0, Schrödinger, LLC, New York, NY, 2009.
- [37] MacroModel, Version 9.7, Schrödinger, LLC, New York, NY, 2009.
- [38] W.C. Still, A. Tempczyk, R.C. Hawley, T. Hendrickson, Semianalytical treatment of solvation for molecular mechanics and dynamics, *Journal of American Chemical Society* 112 (16) (1990) 6127–6129.
- [39] J. Shelley, A. Cholleti, L. Frye, J. Greenwood, M. Timlin, M. Uchimaya, Epik: a software program for pK(a) prediction and protonation state generation for drug-like molecules, *Journal of Computer-aided Molecular Design* 21 (12) (2007) 681–691.
- [40] Prime, Version 2.1, Schrödinger, LLC, New York, NY, 2009.
- [41] Glide, Version 5.5, Schrödinger, LLC, New York, NY, 2009.
- [42] W. Sherman, T. Day, M. Jacobson, R. Friesner, R. Farid, Novel procedure for modeling ligand/receptor induced fit effects, *Journal of Medicinal Chemistry* 49 (2) (2006) 534–553.